ELSEVIER

Contents lists available at ScienceDirect

Applied Catalysis B: Environmental

journal homepage: www.elsevier.com/locate/apcatb





Developing single-site Pt catalysts for the preferential oxidation of CO: A surface science and first principles-guided approach

Jilei Liu^{a,1}, Alyssa J.R. Hensley^{b,1}, Georgios Giannakakis^{a,1}, Andrew J. Therrien^{c,1}, Ahmad Sukkar^a, Alex C. Schilling^c, Kyle Groden^b, Nisa Ulumuddin^b, Ryan T. Hannagan^c, Mengyao Ouyang^a, Maria Flytzani-Stephanopoulos^a, Jean-Sabin McEwen^{b,d,e,f,**}, E. Charles H. Sykes^{c,*}

- a Department of Chemical and Biological Engineering, Tufts University, 4 Colby Street, Medford, MA 02155, USA
- b The Gene and Linda Voiland School of Chemical Engineering and Bioengineering, Washington State University, Pullman, WA 99164, USA
- ^c Department of Chemistry, Tufts University, 62 Talbot Avenue, Medford, MA 02155, USA
- ^d Department of Chemistry, Washington State University, Pullman, WA 99164, USA
- ^e Department of Biological Systems Engineering, Washington State University, Pullman, WA 99164, USA
- f Institute for Integrated Catalysis, Pacific Northwest National Laboratory, Richland, WA 99352, USA

ARTICLE INFO

Keywords: Single-site catalysts CO preferential oxidation Platinum Cuprous oxide

ABSTRACT

We report a comprehensive study combining surface science, Density Functional Theory (DFT) calculations, and catalyst synthesis, characterization, and testing to investigate the preferential oxidation of CO in the presence of H_2 over single-site Pt_1/Cu_xO catalysts. Surface science studies show that while Pt_1/Cu_xO model surfaces enable low-temperature CO oxidation via a Mars-van Krevelen mechanism, there was no evidence for H_2 activation or oxidation. DFT-based calculations explain these results and demonstrate that the H_2 oxidation barrier is high as compared to H_2 desorption from Pt_1/Cu_xO . Inspired by these model catalyst studies, nanoporous Pt_1/Cu_xO catalysts were synthesized and demonstrated to be active and highly selective for the preferential oxidation of CO. This work highlights the potential of combined surface science, theory, and catalyst studies for identifying new catalytic materials, which in this case led to the development of a promising single-site Pt_1/Cu_xO catalyst for the preferential oxidation of CO.

1. Introduction

Single-site catalysts have emerged as a class of promising materials for many important reactions in industry, which include but are not limited to water gas shift, CO oxidation, steam reforming, methane oxidation, selective hydrogenation and dehydrogenation reactions [1–6]. The active precious metals remain isolated and coordinated with oxygen, nitrogen or metallic hosts and exhibit the desirable properties for selective functionalization of chemical bonds, avoiding undesirable pathways. Impressively, their performance is not transient and most of the proposed catalysts exhibit remarkable activity for prolonged periods of time on stream.

Despite the plethora of promising single-site catalysts reported in the

literature, little has been understood regarding the role of the single metal atoms in the reaction mechanism and the true nature of the single atom in practical catalysts [7]. It is therefore important for theoretical investigations and surface science studies on model crystals to educate the design of the catalytic materials, as well as to delineate the nature of the isolated metal atoms and cations [8–10]. Such an approach has yielded impressive results in the case of single-atom alloys (SAAs), a subclass of single-site catalysts [11]. SAAs were designed under ultra-high vacuum (UHV) conditions, implemented in ambient pressure catalysis and understood via theoretical simulations. Their potential to escape linear scaling relations that dictate monometallic and alloy catalysts have gained a lot of attention across the fields of thermal, electroand photo- catalysis, as they yield highly active, stable and selective

^{*} Corresponding author.

^{**} Corresponding author at: The Gene and Linda Voiland School of Chemical Engineering and Bioengineering, Washington State University, Pullman, WA 99164, USA.

E-mail addresses: js.mcewen@wsu.edu (J.-S. McEwen), charles.sykes@tufts.edu (E.C.H. Sykes).

¹ These authors contributed equally to this work.

catalysts for a wide range of reactions [12,13]. These concerted efforts not only provide an in-depth elucidation of the nature of these materials but are also a powerful tool in predicting the behavior and rationally designing the next generation of catalysts [11,12]. It is therefore expected that this three-pronged approach can similarly aid in the development and investigation of the properties of single-site catalysts under CO preferential oxidation (PrOX) conditions.

CO PrOX catalysts are important in industry and are critical for technologies such as polymer-electrolyte membrane fuel cells [14] that require almost complete elimination of CO from H2 streams; CO acting as a potent poison can limit the efficiency of the catalysts [15]. The fundamental studies on single-site catalysts have shed some light on the nature of active sites and the reaction mechanism. It is widely accepted that cationic Pt and Au atoms with neighboring oxygen atoms are the more favorable active sites for those reactions [2,4,16-18]. Initial studies over cationic Pt and Au yielded highly active catalysts that ensured increased selectivity (~50 %) as compared to nanoparticle containing catalysts (~40 %) [4,16]. A recent work by Cao et al. [19] overcame considerably this oxygen selectivity value and reached 70 % at 100 % conversion over oxygen-bonded alkaline ions that stabilize cationic Pt atoms (2 wt.%). Copper based catalysts have also been examined for this reaction and in fact exhibit high catalytic activity toward CO conversion but usually at high temperatures. Cu_xO catalysts have been studied on reducible supports [20] showing promising activity at relatively low temperatures. The capabilities of thin oxide films, namely a Cu₂O/Cu(111)-like layer consisting of six hexagonal oxide rings made up of O— Cu —O bonded networks otherwise known as the "29" Cu oxide has been studied recently extensively, regarding its ability to adsorb atomic H [21], activate CO [22], H₂O, [23] and O₂ [21]. In a recent report, Pt atom doping on this Cu₂O/Cu(111)-like layer resulted in active surfaces for CO oxidation and helped identify the Mars van Krevelen mechanism taking place [8]. It is therefore hypothesized that coupling the capabilities of Cu₂O-like thin films with Pt atoms dispersed on the surface might yield a competitive catalyst for CO oxidation. Further investigations are required to determine whether these surfaces can also combine the weak interaction with H2 and therefore constitute promising candidates for the CO preferential oxidation reaction, combining high activity, stability, and oxygen selectivity.

To that end, the findings from surface science and theoretical studies guide the design and synthesis of catalyst analogs in nanoporous form with thin oxide surface films. The samples are then characterized and tested under CO oxidation and PrOX reaction conditions, exhibiting very good activity, stability and selectivity, in agreement with DFT simulations and UHV studies. Pt-atom doping results in approximately 10 times more active catalysts than pure Cu_xO , while H_2 selectivity is only limited to 5 % at 100 % CO conversion.

2. Methods

2.1. Catalyst preparation

The sacrificial support method was followed for the preparation of all nanoporous copper catalysts [24,25]. Fumed silica (Sigma-Aldrich, 0.15 μm particles size) was treated at 600 °C in static air for 6 h prior to use. Appropriate amounts of Cu precursor (Cu(NO_3)_2) were added by the incipient wetness impregnation method to the silica support. The sample was dried in a vacuum oven for 24 h before being calcined at 300 °C for 3 h. Treatment with concentrated (8 M) KOH solution enabled the silica support to be leached away after 2 h, leaving a nanoporous copper network. This material was then washed until the filtrate was pH-neutral. The resulting nanoporous Cu catalyst was reduced in pure $\rm H_2$ at 250 °C.

The Pt was added to the surface of nanoporous Cu via the galvanic replacement method as reported previously [11,26,27], forming a single-atom alloy. First, the nanoporous Cu was reduced in pure $\rm H_2$ at 250 °C before being transferred to a round bottom flask containing 50

mL of DI water flushed with nitrogen and boiled under reflux. Two drops of dilute (\sim 10 %) HCl were added to ensure an exposed metallic copper surface suitable for galvanic replacement. A solution of chloroplatinic acid was then added dropwise, which corresponded to 0.1 at. % of Pt deposited in the Cu surface. Samples with higher Pt loading (19 at. %) were also prepared for XPS analysis. The number of surface copper atoms in the sample was approximated by using the measured BET surface area. Galvanic replacement was carried out over 5 min. The resulting materials were filtered and washed with DI water until no Cl was detected with AgNO $_3$.

Pre-reduced nanoporous Cu or PtCu catalysts were treated in a 1 M solution of KOH flushed with inert gas for 2 h. The inert gas flow was turned off during the oxidation process to allow a small amount of oxygen to enter the system. In this environment, cuprous oxide is the thermodynamically favorable form of copper and so the metal is partially oxidized. The sample was then retrieved and washed until pH-neutral.

2.2. XRD

X-ray Diffraction (XRD) analysis was performed on a PANalytical X'Pert Pro instrument. Cu $K\alpha$ radiation was used with a power setting of 40 mA, 45 kV. Data was collected for 20 between 10° and 80°. The catalysts were reduced in 100 % H_2 at 250 °C prior to the XRD measurements.

2.3. TEM/SEM

High-resolution transmission electron microscopy (HR-TEM) measurements were conducted on a JEOL 2010 electron microscope with a 200 kV and 107 μA beam. Small amounts of the samples were diluted in ethanol and then drop casted onto lacey carbon on nickel TEM grids. Scanning electron microscope (SEM) images were taken using a Zeiss Supra 55 V P instrument.

2.4. CO-IR

Infrared (IR) spectroscopy was performed in diffuse reflectance infrared Fourier transform spectroscopy (DRIFTS) mode on a Thermo Nicolet iS50 FT-IR. Around 0.05 g of catalyst powder was loaded in the sample cup. The sample was treated in $\rm H_2$ at 250°C in situ, followed by degassing in He at ambient temperature. Pure CO was introduced into the chamber at ambient temperature for 15 min, followed by purging with pure He at the same temperature. The IR spectra were collected at different time points after introduction of CO gas.

2.5. TPO

Temperature programmed oxidation (TPO) experiments were performed in a packed-bed flow microreactor (L = 22 inch, O.D. = 1/2 inch) on the used catalysts. 20 % O₂/He (20 ml/min) was introduced to the reactor and the system was stabilized for one hour. To perform TPO, the temperature was increased from ambient temperature to 600 °C at 3 °C/min. The gas effluent from the reactor was analyzed by a mass-spectrometer following m/z 44, corresponding to CO₂.

2.6. Computational methods

The density functional calculations discussed here were performed with the Vienna *Abinitio* Simulation Package (VASP) [28,29]. The core electrons are described using the Projector Augmented Wave (PAW) [30, 31] method (potentials taken from March 2002 release). The valence electrons are modeled with the Perdew-Burke-Ernzerhof (PBE) [32] functional. A plane wave basis set with an energy cutoff of 500 eV was found to be sufficient, and the electron smearing was described with the Gaussian smearing method with a width of 0.2 eV. All surface

calculations were performed using a (1 \times 2 \times 1) Monkhorst-Pack [33] k-points mesh.

The "29" Cu oxide surface structure was modeled as in our previous studies by putting a Cu₂O-like layer on a 4-layer thick Cu(111) surface (Cu_{metal}) within a $\sqrt{13}R46.1^{\circ} \times 7R21.8^{\circ}$ supercell. The Cu₂O-like layer is made from fused hexagonal rings, each with 6 Cu atoms (Cu_{oxide}) and 6 O atoms (O_{oxide}). There are 6 of these hexagonal rings per "29" oxide unit cell, which has 18 Cu oxide atoms and 12 O oxide atoms in total (Fig. S1). There are also O adatoms (O_{adatom}) in the center of 5 of the 6 rings, which adsorb at hollow sites of the Cu(111) surface where they are bound most strongly. The bottom 2 layers of the slab were kept fixed in their bulk positions, with a lattice constant of 3.635 Å. Full details of the construction and verification of the surface model of "29" oxide support are available in our previous work [22,34,35].

Each ground-state optimization calculation was considered converged when the total energy changed by less than 10^{-6} eV, and the forces between atoms were smaller than $0.02 \, \mathrm{eV/\mathring{A}}$. The transition states were investigated using first the nudged elastic band (NEB) [36] method to pre-converge the minimum energy pathway (MEP) to a total energy accuracy of 10^{-4} eV and interatomic forces of less than $0.1 \, \mathrm{eV/\mathring{A}}$. This MEP was then converged using the climbing image nudged elastic band (CINEB) [37] method to total energy accuracy of $10^{-6} \, \mathrm{eV}$ and interatomic forces of less than $0.03 \, \mathrm{eV/\mathring{A}}$. The presence of a transition state was verified by calculating the vibrational modes for the highest energy structure in the CINEB optimized MEP and ensuring that there was a single imaginary mode along the reaction pathway [38].

The adsorption energies for atomic H and molecular H_2 on "29" Cu oxide were calculated according to:

$$E_{\text{ads}}^{\text{atomicH}} = E_{\text{H/oxide}} - E_{\text{oxide}} - \frac{1}{2} E_{\text{H}_2}$$
 (1)

$$E_{\text{ads}}^{\text{molecularH}_2} = E_{\text{H}_2/\text{oxide}} - E_{\text{oxide}} - E_{\text{H}_2} \tag{2}$$

where $E_{\rm H/oxide}$, $E_{\rm H_2/oxide}$, $E_{\rm oxide}$, and $E_{\rm H_2}$ are the total energies of atomic H adsorbed on "29" Cu oxide, molecular H₂ adsorbed on "29" Cu oxide, the "29" Cu oxide surface, and gas phase H₂. The adsorption energy for CO on the "29" Cu oxide was calculated by:

$$E_{\text{ads}}^{\text{CO}} = E_{\text{CO/oxide}} - E_{\text{oxide}} - E_{\text{CO}} \tag{3}$$

Where $E_{\rm CO/oxide}$ and $E_{\rm CO}$ are the total energies of CO adsorbed on "29" Cu oxide and gas phase CO.

As inclusion of temperature and pressure effects are most significant for adsorption steps due to the loss of translation and rotational degrees of freedom for the surface bound molecule, we calculated the Gibbs adsorption energies for molecular H_2 and CO according to:

$$\Delta G_{\rm ads}^{\rm M} = E_{\rm ads}^{\rm M} + \Delta G_{\rm M/oxide} - \Delta G_{\rm oxide} - \Delta G_{\rm M} \tag{4}$$

$$\Delta G_{\rm M/oxide} = -k_{\rm B}T \ln \left(q_{\rm vibs}^{\rm M/oxide}\right) \tag{5}$$

$$\Delta G_{\text{oxide}} = -k_{\text{B}} T \ln(q_{\text{vibs}}^{\text{oxide}}) \tag{6}$$

$$\Delta G_{\rm M} = -k_{\rm B} T \ln \left(q_{\rm vibs}^{\rm M} q_{\rm rot}^{\rm M} q_{\rm trans}^{\rm M} \right) \tag{7}$$

where $\Delta G_{\mathrm{M/oxide}}$, $\Delta G_{\mathrm{oxide}}$, and ΔG_{M} are the Gibbs energy corrections for the adsorbate covered surface, surface alone, and gas phase molecule; $q_{\mathrm{vibs}}^{\mathrm{M/oxide}}$, $q_{\mathrm{vibs}}^{\mathrm{oxide}}$, $q_{\mathrm{vibs}}^{\mathrm{M}}$, $q_{\mathrm{rot}}^{\mathrm{M}}$, and $q_{\mathrm{trans}}^{\mathrm{M}}$ are the partition functions for the vibrations of the adsorbate covered surface, vibrations of the surface alone, and vibrations, rotations, and translations of the gas phase molecule; k_{B} and T are Boltzmann's constant and temperature. The partition functions were calculated according to:

$$q_{\text{vibs}}^{i} = \prod_{j=1}^{N_{\text{modes}}^{i}} \frac{\exp\left(-\frac{hv_{j}^{i}}{2k_{\text{B}}T}\right)}{1 - \exp\left(-\frac{hv_{j}^{i}}{k_{\text{B}}T}\right)}$$
(8)

$$q_{\text{rot}}^{i} = \frac{8\pi^{2}\mu_{i}R_{i}^{2}k_{\text{B}}T}{\sigma_{i}h^{2}} \tag{9}$$

$$q_{\text{trans}}^{i} = \left(\frac{2\pi m_{i} k_{\text{B}} T}{h^{2}}\right)^{\frac{3}{2}} * \frac{k_{\text{B}} T}{P_{i}}$$
 (10)

where h is Plank's constant; v_j^i , N_{modes}^i , μ_i , R_i , σ_i , m_i , and P_i are the j^{th} vibrational mode, number of vibrational modes, reduced mass, bond length, symmetry number, total mass, and partial pressure of the i^{th} species.

2.7. Flow reactor studies

To perform the Temperature Programmed Surface Reaction (TPSR) studies, typically, 0.5 g of nanoporous cuprous oxide catalysts – Pt_1/Cu_xO and the control Cu_xO - were loaded into the reactor. For CO oxidation studies, a 2 % CO, 2 % O_2 and balanced in a He mixture that was introduced with a total flow rate of 50 ml/min. The reactions were run with a temperature ramp of 1°C / min from room temperature (27°C) up to 180°C and held there for 20 min. The temperature was then lowered at the same rate of 1 °C / min down to room temperature again and given time to attain equilibrium before a new cycle was run. The gas composition was analyzed with a micro-GC. At least three cycles of CO oxidation were run for each set of conditions. The PrOX reactions were conducted with the same reactor set up. The gas composition was 2 % O_2 , 2 % CO, 40 % H_2 , balance He. Conversion was calculated from oxygen peak area data at each temperature using a recent GC calibration for oxygen.

2.8. Ultra-high vacuum studies

2.8.1. Scanning tunneling microscopy

The scanning tunneling microscopy (STM) images presented in this study were obtained from a Cu(111) single crystal prepared in a preparation chamber with a base pressure of 2×10^{-10} mbar. The sample preparation consisted of cleaning \emph{via} Ar^+ sputtering followed by annealing to 750 K. To make the "29" oxide film the clean surface was exposed to O_2 gas (USP Grade; Airgas) at a pressure of 5×10^{-6} mbar for 3 min with a sample temperature of 650 ± 20 K. The "29" oxide structure was then verified with a low energy electron diffraction (LEED) apparatus (OCI Vacuum Microengineering). Pt was deposited at 85 K, using a Focus GmbH EFM3 electron beam evaporator. The sample was then transferred in vacuum to an Omicron Technology low-temperature ultra-high vacuum (LT-UHV) STM (base pressure 1×10^{-11} mbar) for imaging. The Pt coverage was determined by defining one monolayer as the packing density of Cu(111), 1.77×10^{15} atoms cm $^{-2}$.

2.8.2. Temperature programmed desorption

The temperature programmed desorption (TPD) experiments presented here were performed in an ultra-high vacuum (UHV) chamber with a base pressure of $<1\times10^{-10}$ mbar. The sample preparation procedure was the same as the STM experiments. The Cu(111) crystal could be cooled to 85 K with liquid nitrogen, and resistively heated to 750 K. High precision leak valves enabled reproducible exposure to CO (99.99 %; Airgas), H₂ (99.9 %; Airgas), and D₂ (99.99 %; Airgas) gas depending on the experiment. After gas deposition the sample was aligned with a quadrupole mass spectrometer (Hiden) and the crystal was heated at a linear heating rate of 1 K/s. Fragmentation pattern, ionization cross section, and quadrupole mass spectrometer sensitivity were accounted for in all TPD traces presented.

3. Results and discussion

3.1. Model studies on the "29" Cu oxide

To investigate the activity, selectivity and reaction mechanism of single-site Pt on Cu_xO catalysts in the PrOX reaction, a surface science approach was first taken. The single layer "29" Cu oxide surface on Cu (111) served as a model for Cu_2O [35]. Pt atoms are deposited onto the "29" Cu oxide surface at 85 K followed by annealing to 250 K which allows the Pt atoms to equilibrate at their favored binding site on the oxide support [8]. The surface was characterized by scanning tunneling spectroscopy (STM), shown in Fig. 1A. The Pt atoms, seen as bright protrusions in STM images, are mono-disperse on the surface, as evidenced by their uniform size and shape. The corrugation of the "29" Cu oxide can be seen in Fig. 1, and most Pt atoms occupy identical sites with respect to the unit cell of the oxide surface [8].

The activity of Cu₂O supported single Pt atoms toward the PrOX reaction was investigated by temperature programed desorption (TPD). In order to ascertain if the model surface was able to activate molecular hydrogen, hydrogen was deposited at 85 K and TPD used to look for recombinative desorption of H₂ or water formation. In order to deconvolute reactively formed water from background water in the chamber, experiments were also performed in which the surface was exposed to D₂ so that reactively formed D₂O could be detected The surface was exposed to 100 L of D₂ (Langmuir, 1 L = 1 \times 10⁻⁶ Torr·s) at 85 K, and the TPD results are shown in Fig. 1B. 100 L of D₂ is sufficient to saturate Pt/Cu single-atom alloy surfaces [8], however no desorption products were observed from the Pt/"29" Cu oxide model surface up to 550 K, suggesting that either (1) D₂ is not activated or (2) D atoms bind too weakly to the surface to be detected desorbing above 85 K.

DFT calculations were performed to probe the MEP for H_2 activation on both the "29" Cu oxide and Pt/ "29" Cu oxide surfaces. Beginning by examining the adsorption of atomic H on the "29" Cu oxide at all possible O and Cu sites [8,22,34,35], it is clear that the O sites—both O_{oxide} and O_{adatom} —are vastly preferred with an average adsorption energy of ~ -0.6 eV as compared ~ 0.4 eV for Cu sites (Fig. S1 and Table S1). The positive adsorption energy for atomic H on Cu sites is even true for the tested Cu_{metal} sites which have adsorption energies of ~ 0.3 eV. This unfavorable bonding of H to the Cu(111) surface is likely due to the fact that the first layer of Cu in the Cu(111) surface is positively charged [34]. As a consequence of the highly unfavorable interaction between atomic H and the Cu sites, H diffusion across the surface is predicted here to be nearly non-existent with reaction energies of over 1 eV for traversing over Cu atoms between O sites.

To have atomic H present on the "29" Cu oxide, H₂ must either (1) molecularly adsorb to the surface with an adsorption strength that is

competitive with the activation barrier for dissociation or (2) undergo facile dissociative adsorption. Molecular H_2 adsorption was examined exclusively atop O sites on the "29" Cu oxide with Cu sites being discarded as possibilities due to their weak atomic H adsorption energies (Fig. S1 and Table S1). Even at the most favorable adsorption site, where the adsorption energy is -0.07 eV, the H_2 molecule lifts off of the surface (H_2 – O_{oxide} distance is 3.1 Å), showing that H_2 does not adsorb molecularly. Thus, only facile dissociative H_2 adsorption remains as a possible route for the formation of atomic H on "29" Cu oxide.

As shown in Fig. 2A, H_2 dissociative adsorption onto the "29" Cu oxide is a highly energy intensive process and is, thus, predicted here to not occur. To dissociate molecular H_2 on the "29" Cu oxide, H_2 must first become preferentially trapped beneath a Cu_xO ring with an associated energy cost of 1.8 eV. Once trapped, H_2 easily dissociates (Fig. 2A, TS1) in a hugely exothermic reaction (-3.1 eV) to form two adsorbed H atoms on adjacent O_{oxide} and O_{adatom} sites. Despite the thermodynamically favorable final state of adsorbed atomic H, the significant energy cost of bringing H_2 into contact with "29" Cu oxide suggests that this surface will be inactive for H_2 activation, consistent with H_2 TPD experiments performed on this system (Fig. 1B).

The activation of H₂ over Pt single atoms supported on the "29" Cu oxide surface was studied via DFT using the model developed in our previous work on the low temperature oxidation of CO [8], and the results are shown in Fig. 2A. Different from the "29" Cu oxide, H2 binds weakly to the Pt single atom, easily dissociating to 2H bound to the Pt atom (Fig. 2A, TS2) with a binding strength of -0.1 eV. The next step in the H₂ oxidation reaction is the transfer of adsorbed H to an adjacent oxygen to form first OH and then H2O. The first H diffusion step is exothermic (-0.7 eV) with a barrier of 0.7 eV for H adatom diffusion from Pt to the O_{oxide} site. Diffusion of the second H to the O_{oxide}, forming two OH groups, is further exothermic by -0.2 eV, consistent with the recent work by Doudin et al. for H2 activation on Pd single atoms on Fe₃O₄(001) [39]. An additional pathway involving the heterolytic cleavage of H2 to 2H upon adsorption was tested, but this pathway does not occur as the transition state calculation converged to an intermediate minimum with H2 adsorbed on the Pt atom, similar to the results shown in Fig. 2A.

As compared to H_2 recombination and desorption, which has an effective energy cost of 0.1 eV, H diffusion onto the O_{oxide} , and thus oxidation, has a significantly higher energy cost of 0.7 eV. In fact, a comparison of Boltzmann probabilities for both steps $\left[\exp\left(-\frac{\left(\Delta E_{recomb} + desorp - \Delta E_{diff}\right)}{k_BT}\right)\right]$ at T=85 K, the experimental H_2 dosing temperature, shows that H_2 recombination and desorption is $\sim 10^{35}$ times faster than H diffusion. Furthermore, calculation of the Gibbs adsorption

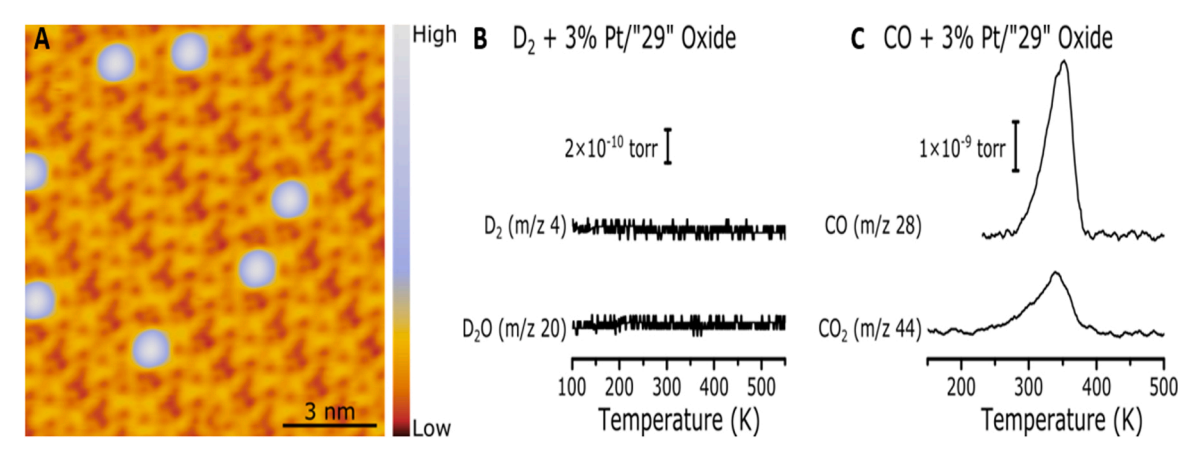


Fig. 1. Model study investigation of 3 % ML of Pt supported on the "29" Cu surface oxide toward CO and hydrogen oxidation. A) STM image of single Pt atoms supported on the "29" oxide Cu_2O surface following a 250 K anneal. Imaging conducted at 5 K at conditions of -0.45 V, 1 nA. TPD results following exposure to B) 100 L D_2 and C) 10 L CO. TPD traces are offset for clarity.

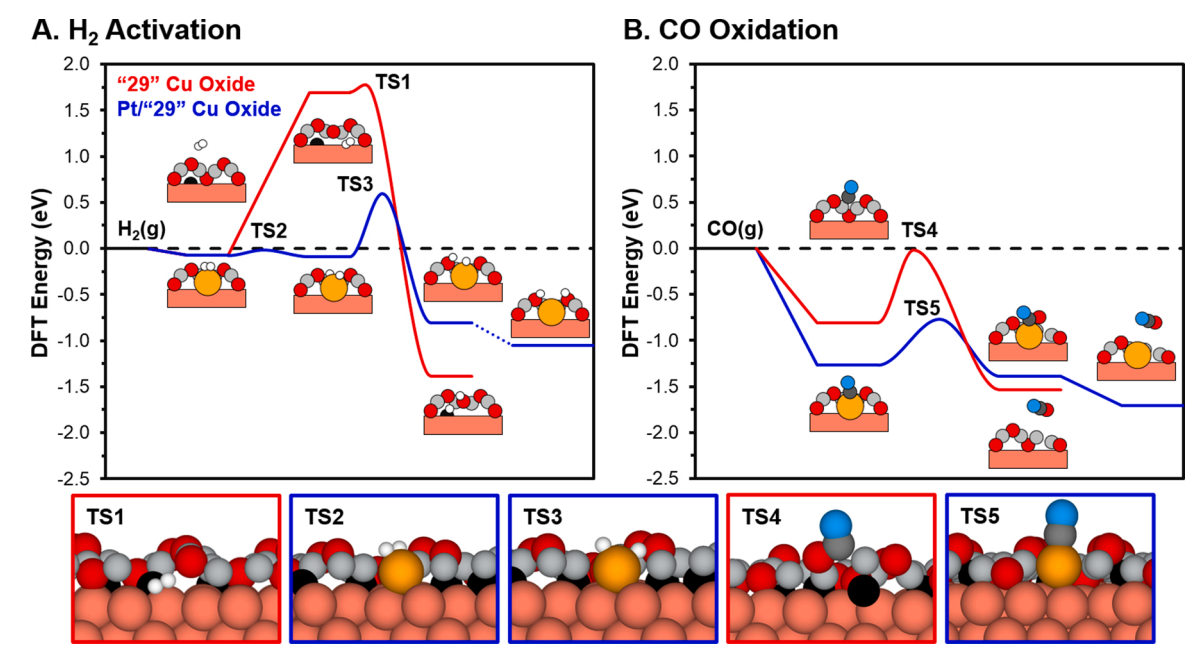


Fig. 2. Minimum energy pathways for H_2 activation (A) and CO oxidation (B) on the "29" Cu oxide and the Pt/"29" Cu oxide. The respective clean surfaces and H_2 or CO in the gas phase were used as energy reference. The data for CO oxidation on Pt/"29" Cu oxide has been taken from Ref. [8]. Side views of the calculated transition states (TS) are shown below, with more details shown in Fig. S2. The pink, silver, gold, red, black, grey, light blue, and white spheres represent Cu_{metab} Cu_{oxide} , Pt, O_{oxide} , O_{oxide}

energy for H_2 adsorption is always positive on both the "29" oxide and Pt/"29" oxide (Fig. 3A) for pressures below 250 bar, showing that gas phase H_2 is highly favored over molecularly adsorbed H_2 . Therefore, molecular H_2 adsorption and subsequent dissociation on the Pt single atom site is unlikely to occur under a wide range of conditions, making the presence of surface H that can diffuse from Pt to O_{oxide} sites, and subsequently oxidize, significantly less likely than H_2 desorption. Overall, this work shows that the Pt/"29" Pt/ Cu oxide surface is likely inactive for Pt/ oxidation, making this surface a good candidate for the Pt/ of Pt/ CO reaction.

Activity toward CO oxidation was investigated via TPD in a similar way to $\rm H_2$ oxidation. The 3 % Pt "29" oxide surface was exposed to 10 L of CO, and the resulting TPD traces are shown in Fig. 1C. Unlike the $\rm D_2$ results, CO and the oxidized product $\rm CO_2$ desorption is observed desorbing below 350 K. CO and $\rm CO_2$ desorption occur at similar temperatures in a 2:1 ratio. Isotope labelling experiments have shown that the oxidation of CO by single Pt atoms on this oxide surface proceeds via a Mars-van Krevelen mechanism in which the oxygen for CO oxidation is supplied by the 29 oxide [8].

By comparing to our previous work modeling the MEP for CO oxidation by a Mars-van Krevelen mechanism on Pt/"29" Cu oxide (Fig. 2B), it is clear that CO oxidation is the energetically preferred pathway over H₂ activation (Fig. 2A) [8]. Beginning with adsorption, CO adsorbs to the Pt single atom with an adsorption energy of -1.3 eV and, thus, will outcompete H2 dissociation, which has an adsorption energy of -0.1 eV, for binding to the Pt sites. This is further demonstrated by calculating the Gibbs adsorption energy for CO on the Pt single atom (Fig. 3B), which shows that the CO binds stronger to the Pt single atom than H₂ by 0.7–1.1 eV depending on the temperature. Progressing along the reaction coordinate, the Pt bound CO molecule reacts with an O_{oxide} species in a concerted step where the new O=C···Ooxide bond forms and several $Cu_{oxide} \cdots O_{oxide}$ bonds break in the same step (Fig. 2B, TS4). This step has a moderate activation energy of 0.5 eV. The remaining step of CO2 desorption is exothermic. A direct comparison of the H2 activation and CO oxidation pathways shows that just the adsorption of CO onto the Pt single atom site releases more energy than that of H₂ adsorption,

dissociation, and diffusion to an O_{oxide} site combined (i.e. -1.3 eV versus -1.1 eV, respectively). Finally, we note that the presence of the Pt adatom is necessary here with regard to CO oxidation since it anchors the CO to the "29" oxide surface. Indeed, in Fig. 2B and Fig. 3B, CO will likely desorb from the oxide surface rather than oxidize to form CO_2 on the bare "29" oxide. On the other hand, in the presence of a Pt atom, the desorption of CO is much less likely since CO binds more strongly to the Pt adatom as compared to the bare oxide surface allowing it to react. Taken together, these results predict that the Pt/"29" Cu oxide interface shows great promise for PrOX activity if present in a working catalyst.

3.2. Catalysis studies

3.2.1. Catalyst characterization

Guided by the predictions from theory and surface science results, the catalyst analogs were prepared in nanoporous form. To that end, the sacrificial support method [40] was employed. This method has proven useful for the synthesis of unsupported materials, an approach that has been effective in removing the effect of the support and delineating the role of metals in single-atom alloys [24,25]. The successful formation of a porous structure was verified via BET, which indicates that the surface has an area of 10 m²/g. Further information on the nanoporous nature of copper oxide materials arise from SEM images that depict particle beads in the range of $\sim\!0.25~\mu m$ (Fig. S3). XRD analysis of the fresh material indicates that highly crystalline metallic Cu with {111}, {200}, and {220} facets are formed during the catalyst synthesis (Fig. 4a). The Cu₂O phase was also observed with peaks at 36 and 44 degrees, corresponding to {111} and {200} planes respectively [41,42], which is likely due to the formation of the surface oxide layer. After reaction, it is clear that the {111} plane is the most prevalent of Cu₂O. This is consistent with several theoretical studies in the literature, where an oxygen-terminated Cu₂O {111} surface was found to be one of the most energetically stable facets [43-46]. TEM images corroborate the XRD results in that highly crystalline phases were observed with lattice spacing equal to 0.25 nm (Fig. 4c), characteristic of Cu₂O {111} planes exposed on the surface [47]. The atomic dispersion of Pt in Cu has previously been confirmed

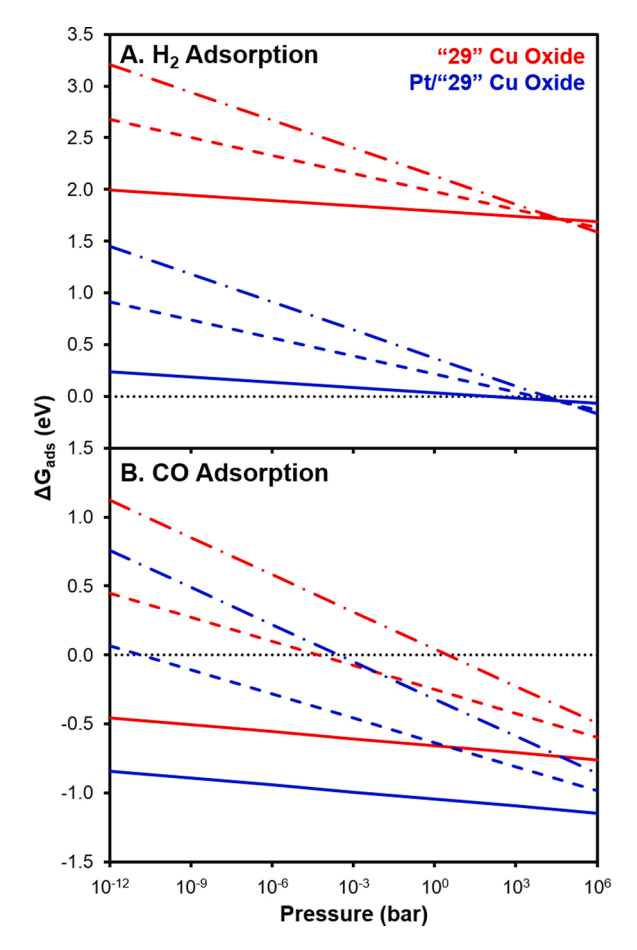


Fig. 3. Gibbs adsorption energy for (A) $\rm H_2$ (40 mol%) and (B) CO (2 mol%) on the "29" oxide and the Pt/"29" oxide as a function of total pressure at temperatures of 85 K (solid line), 293 K (dashed line), and 453 K (dot dashed line). The data for CO oxidation on Pt/"29" Cu oxide has been taken from Ref. [8].

with various characterization techniques [27,48,49]. Here we conducted CO-DRIFTS, which clearly shows the absence of bridge bound CO and only yields a peak centered at 2097 cm⁻¹. CO stretches at this frequency have been attributed to CO binding to a positively charged single Pt atom on CeO₂ in the literature (Fig. 4b) [50]. To further investigate the charge of the Pt sites, XPS measurements were conducted. However the analysis of this data is challenging because of the very low signal-to-noise ratio of the Pt 3d peak due to the low concentration of Pt on the Pt₁/Cu_xO catalyst. Additionally, Pt 4f XPS peaks overlap with Cu 3p peaks from the support Cu_xO, which made data interpretation difficult. To overcome those issues, a $PtCu_xO$ catalyst with around 100 times higher Pt concentration than Pt₁/Cu_xO was synthesized and characterized with XPS. It is clear from Fig. S4 that the average binding energy of the Pt $4d_{5/2}$ peak is slightly higher than that of metallic Pt (black dash lines) and consistent with reported binding energy values of positively charged Pt. This suggests that in addition to the metallic Pt nanoparticles present due to the high Pt loading, that there is also cationic Pt species. This result, coupled with the CO DRIFTS peak (Fig. 4b) which has a high wavenumber, indicate that low loadings of Pt on Cu_vO are positively charged.

3.2.2. Flow reactor studies

Following the synthesis and characterization of the desired single atom Pt₁/Cu_xO structure, the CO oxidation reactivity of the catalyst was investigated. It is clear that the addition of Pt atoms to CuxO improves the CO oxidation activity (Fig. 5a). At a CO:O2 ratio of 1:1, the light-off temperature of CO oxidation decreases by 50 °C as compared to pure Cu_xO. The improvement in reactivity is apparent when comparing the conversion at 100 °C, at which point Pt₁/Cu_xO is measured to be approximately 10 times more active than bare CuxO. The single-site Pt catalysts show remarkable stability for 30 h on stream under these conditions (Fig. S5), not losing their initial reactivity. A TPO analysis on this sample indicates small amounts of carbon deposition, similar to that on pure Cu_xO (Fig. S6). While CO poisoning is known to be a challenging issue on extended Pt surfaces [27], this does not seem to be an issue for Pt₁/Cu_xO. This interesting behavior of the Pt₁/Cu_xO catalyst is the result of weak interaction between atomically dispersed Pt and CO, in agreement with previously reported CO tolerance of PtCu SAAs [27]. Under stoichiometric ratios of CO:O2 (2:1) the difference in light-off temperatures is maintained between Pt₁/Cu_xO and Cu_xO, reaffirming the

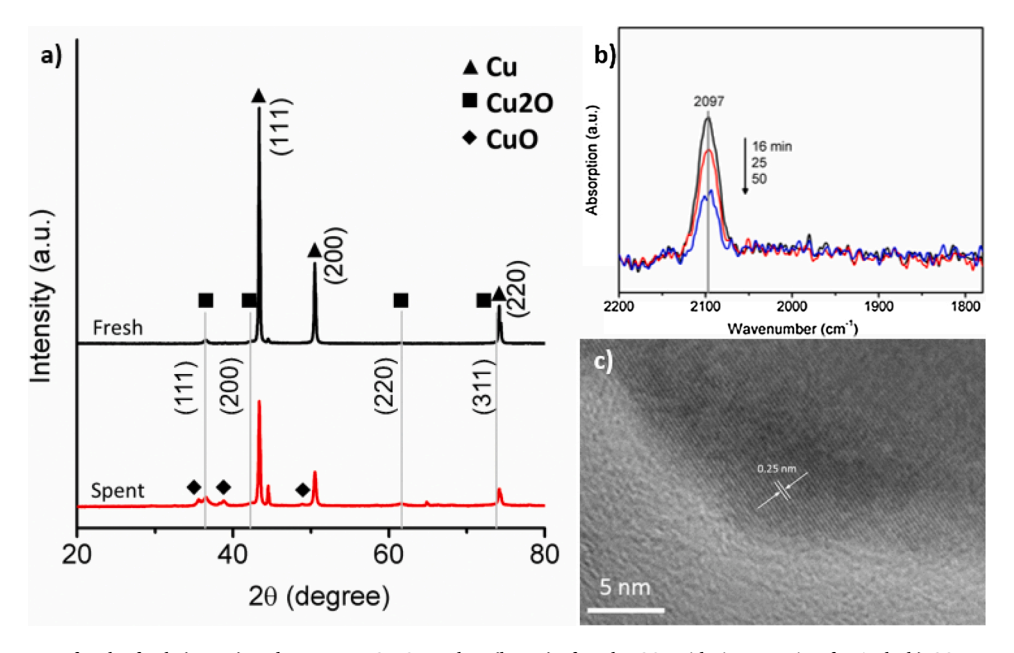


Fig. 4. a) XRD measurements for the fresh (upper) and spent Pt_1/Cu_xO catalyst (lower) after the CO oxidation reaction for 15 h. b) CO DRIFTS of fresh Pt_1/Cu_xO c) TEM image of as prepared Pt_1/Cu_xO .

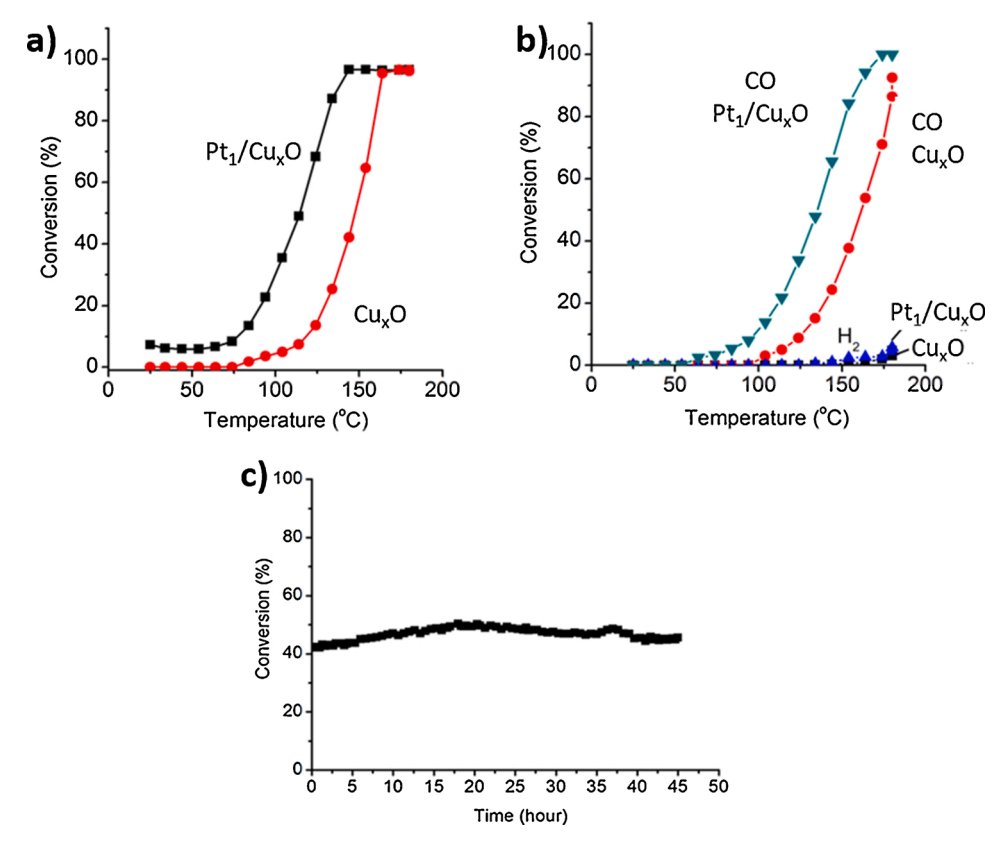


Fig. 5. a) Second cycle TPSR data for CO oxidation over Pt_1/Cu_xO and Cu_xO catalysts, flow rate: 50 mL/min, 2 % O_2 , 2 % CO, bal. He, 500 mg samples b) Temperature Programmed PrOX reaction on Pt_1/Cu_xO and Cu_xO catalysts, flow rate: 50 mL/min, 2 % O_2 , 2 % CO, 40 % H_2 , bal. He, 500 mg sample c) Steady-state PrOX at 130°C over Pt_1/Cu_xO , flow rate: 50 mL/min, 2 % O_2 , 2 % CO, 40 % H_2 , bal. He, 250 mg sample.

beneficial effect of Pt atom decoration under these conditions as well (Fig. S7). However, the reactivity of the catalysts is seemingly affected by the amount of oxygen present, as oxygen-lean conditions result in lower conversion over Pt₁/Cu_xO (Fig. S8). Therrien et al. identified a Mars-van Krevelen mechanism of CO oxidation on Pt₁/Cu_xO surface [8]. The oxygen atoms in close vicinity to single-site Pt atoms participate in the oxidation of CO, which rationalizes the catalyst reactivity dependence on the CO:O2 ratio in the feed. Interestingly, Soon et al. [43] found that the Cu₂O(111) facet is the most thermodynamically stable facet under oxygen-lean conditions while the Cu₂O(110) facet was the most thermodynamically stable under oxygen-rich conditions. As such, it is possible that the catalytic activity is correlated to the thermodynamic stability of a given facet, such that the morphology of the nanoparticle dynamically changes as the reaction conditions are varied. This could explain the change in the reactivity of the catalyst under CO rich conditions (Fig. S9) over different cycles. Moreover, while the catalyst is active at low temperatures in the 1st cycle, in the consecutive cycles the CO conversion drops below 100 % as seen in Fig. S9. This is expected, as at such oxygen-lean CO:O2 (4:1) ratios the conversion should not reach 100 %. The fact that 100 % conversion is reached in the initial cycles indicates that surface O atoms from the support (Cu_xO) must participate and is consistent with the Mars-van Krevelen mechanism described. The correlation between reactivity and oxygen partial pressure is also in agreement with previous literature on Pt catalysts supported on γ-Al₂O₃ [51] and CeO₂ [52], as well as on CuO/CeO₂ at stoichiometric reactants ratio and below [53].

The Pt_1/Cu_xO catalyst was highly active and stable at moderate temperatures (Fig. 5c) and over different reactant ratios. While Pt-based catalysts have proven to be active, high oxygen selectivity is still an issue for most of the catalysts featuring contiguous Pt sites [54]. Interestingly, Pt_1/Cu_xO demonstrated excellent selectivity under PrOX conditions, which was maintained throughout the temperature range and even at

100 % conversion of CO (Fig. 5b). Even at the highest temperature tested, the conversion of H_2 to H_2O remained below 5 %. This indicates a preference of the Pt atom to leave the H_2 intact, while retaining its high reactivity to CO oxidation, in agreement with our surface science and DFT-based investigations. The oxygen selectivity to CO_2 was retained at 63 % at full CO conversion, similar to values reported over single-site Au [16] and Pt [4] catalysts (ranging between 50 and 70 %).

4. Conclusions

Using an integrated surface science, catalysis and DFT approach we discovered that atomically dispersed Pt atoms in the surface of Cu_xO are active for CO oxidation, while at the same time, they do not catalyze the oxidation of H2. In addition to their significance for the preferential oxidation of CO reaction, these results shed some light on the recent debate of if single Pt atoms on metal oxide supports are active for CO oxidation [4,55], as we find that single Pt atom doping yielded a remarkable improvement in reactivity. Interestingly, although the presence of Pt does reduce the activation barrier for H₂ dissociation, our DFT-based modeling clearly shows that it is still much more energetically unfavorable to activate H2 as compared to oxidizing CO in the presence of Pt, which helps explain the impressive performance of our nanoporous Pt₁/Cu_xO catalysts which are active and highly selective for the preferential oxidation of CO. We plan to continue using this integrated approach for understanding catalytic sites and reaction mechanisms and our future studies will move beyond the "29" CuxO and focus on Pt atoms on Cu₂O(111) thereby allowing us to interrogate how the charge state of Pt affects reaction pathway [8-10]. We anticipate that such systems will be even more challenging to model from a computational perspective given that hybrid functionals are usually more reliable than the DFT + U method in accurately capturing the electronic structure of a fully oxidized surface. As such, the integration between surface science, theory and catalytic testing will be even more necessary to make further advances toward the development of catalysts than minimize the use of precious metals toward the single atom limit.

CRediT authorship contribution statement

Jilei Liu: Conceptualization, Methodology, Investigation, Writing original draft, Writing - review & editing, Visualization. Alyssa J.R. Hensley: Conceptualization, Investigation, Methodology, Software, Writing - original draft, Writing - review & editing, Visualization. Georgios Giannakakis: Conceptualization, Validation, Investigation, Writing - original draft, Writing - review & editing, Visualization. Andrew J. Therrien: Investigation, Visualization. Ahmad Sukkar: Investigation, Visualization. Alex C. Schilling: Investigation. Kyle Groden: Investigation, Software, Visualization. Nisa Ulumuddin: Investigation. Ryan T. Hannagan: Investigation. Mengyao Ouyang: Investigation. Maria Flytzani-Stephanopoulos: Conceptualization, Supervision. Jean-Sabin McEwen: Conceptualization, Writing - original draft, Writing - review & editing, Resources, Supervision, Funding acquisition. E. Charles H. Sykes: Conceptualization, Writing - original draft, Writing - review & editing, Resources, Supervision, Project administration, Funding acquisition.

Declaration of Competing Interest

The authors report no declarations of interest.

Acknowledgments

Financial support of the experimental work at Tufts by the DOE/BES under Grant # DE-SC0021196 is gratefully acknowledged. Financial support at WSU was provided by the National Science Foundation CAREER program under contract No. CBET-1653561. A portion of the computer time for the computational work was performed using EMSL, a national scientific user facility sponsored by the Department of Energy's Office of Biological and Environmental Research and located at PNNL. PNNL is a multi-program national laboratory operated for the US DOE by Battelle.

Appendix A. Supplementary data

Supplementary material related to this article can be found, in the online version, at doi:https://doi.org/10.1016/j.apcatb.2020.119716.

References

- [1] M. Yang, S. Li, Y. Wang, J.A. Herron, Y. Xu, L.F. Allard, S. Lee, J. Huang, M. Mavrikakis, M. Flytzani-Stephanopoulos, Catalytically active Au-O(OH)_χspecies stabilized by alkali ions on zeolites and mesoprous oxides, Science 346 (2014) 1498–1501.
- [2] S. Cao, M. Yang, A.O. Elnabawy, A. Trimpalis, S. Li, C. Wang, F. Göltl, Z. Chen, J. Liu, J. Shan, M. Li, T. Haas, K.W. Chapman, S. Lee, L.F. Allard, M. Mavrikakis, M. Flytzani-Stephanopoulos, Single-atom gold oxo-clusters prepared in alkaline solutions catalyse the heterogeneous methanol self-coupling reactions, Nat. Chem. 11 (2019) 1098–1105, https://doi.org/10.1038/s41557-019-0345-3.
- [3] J. Shan, M. Li, L.F. Allard, S. Lee, M. Flytzani-Stephanopoulos, Mild oxidation of methane to methanol or acetic acid on supported isolated rhodium catalysts, Nature 551 (2017) 605–608, https://doi.org/10.1038/nature24640.
- [4] B. Qiao, A. Wang, X. Yang, L.F. Allard, Z. Jiang, Y. Cui, J. Liu, J. Li, T. Zhang, Single-atom catalysis of CO oxidation using Pt₁/FeO_x, Nat. Chem. 3 (2011) 634–641, https://doi.org/10.1038/nchem.1095.
- [5] S.K. Kaiser, E. Fako, G. Manzocchi, F. Krumeich, R. Hauert, A.H. Clark, O. V. Safonova, N. López, J. Pérez-Ramírez, Nanostructuring unlocks high performance of platinum single-atom catalysts for stable vinyl chloride production, Nat. Catal. 3 (2020) 376–385, https://doi.org/10.1038/s41929-020-0431-3.
- [6] M.D. Marcinkowski, M.T. Darby, J. Liu, J.M. Wimble, F.R. Lucci, S. Lee, A. Michaelides, M. Flytzani-Stephanopoulos, M. Stamatakis, E.C.H. Sykes, Pt/Cu single-atom alloys as coke-resistant catalysts for efficient C-H activation, Nat. Chem. 10 (2018) 325–332, https://doi.org/10.1038/NCHEM.2915.
- [7] G.S. Parkinson, Single-atom catalysis: how structure influences catalytic performance, Catal. Lett. 149 (2019) 1137–1146, https://doi.org/10.1007/ s10562-019-02709-7.

- [8] A.J. Therrien, A.J.R. Hensley, M.D. Marcinkowski, R. Zhang, F.R. Lucci, B. Coughlin, A.C. Schilling, J.-S. McEwen, E.C.H. Sykes, An atomic-scale view of single-site Pt catalysis for low-temperature CO oxidation, Nat. Catal. 1 (2018) 192–198, https://doi.org/10.1038/s41929-018-0028-2.
- [9] R. Bliem, J.E.S. van der Hoeven, J. Hulva, J. Pavelec, O. Gamba, P.E. de Jongh, M. Schmid, P. Blaha, U. Diebold, G.S. Parkinson, Dual role of CO in the stability of subnano Pt clusters at the Fe₃O₄(001) surface, Proc. Natl. Acad. Sci. U. S. A. 113 (2016) 8921–8926, https://doi.org/10.1073/pnas.1605649113.
- [10] M.D. Marcinkowski, S.F. Yuk, N. Doudin, R.S. Smith, M.T. Nguyen, B.D. Kay, V. A. Glezakou, R. Rousseau, Z. Dohnálek, Low-temperature oxidation of methanol to formaldehyde on a model single-atom catalyst: Pd atoms on Fe₃O₄(001), ACS Catal. 4 (2019) 10977–10982, https://doi.org/10.1021/acscatal.9b03891.
- [11] G. Giannakakis, M. Flytzani-Stephanopoulos, E.C.H. Sykes, Single-atom alloys as a reductionist approach to the rational design of heterogeneous catalysts, Acc. Chem. Res. 52 (2019) 237–247, https://doi.org/10.1021/acs.accounts.8b00490.
- [12] M.T. Darby, M. Stamatakis, A. Michaelides, E.C.H. Sykes, Lonely atoms with special gifts: breaking linear scaling relationships in heterogeneous catalysis with single-atom alloys, J. Phys. Chem. Lett. 9 (2018) 5636–5646, https://doi.org/ 10.1021/acs.inclett.8b01888.
- [13] R.T. Hannagan, G. Giannakakis, M. Flytzani-Stephanopoulos, E.C.H. Sykes, Singleatom alloy catalysis, Acc. Chem. Res. 120 (2020) 12044–12088, https://doi.org/ 10.1021/acs.chemrev.0c00078.
- [14] J.J. Baschuk, X. Li, Carbon monoxide poisoning of proton exchange membrane fuel cells, Int. J. Energy Res. 25 (2001) 695–713, https://doi.org/10.1002/er.713.
- [15] X. Cheng, Z. Shi, N. Glass, L. Zhang, J. Zhang, D. Song, Z.S. Liu, H. Wang, J. Shen, A review of PEM hydrogen fuel cell contamination: impacts, mechanisms, and mitigation, J. Power Sources 165 (2007) 739–756, https://doi.org/10.1016/j. jpowsour.2006.12.012.
- [16] B. Qiao, J. Liu, Y.G. Wang, Q. Lin, X. Liu, A. Wang, J. Li, T. Zhang, J. Liu, Highly efficient catalysis of preferential oxidation of CO in H₂-rich stream by gold singleatom catalysts, ACS Catal. 5 (2015) 6249–6254, https://doi.org/10.1021/ acscatal.5b01114.
- [17] L. Cao, W. Liu, Q. Luo, R. Yin, B. Wang, J. Weissenrieder, M. Soldemo, H. Yan, Y. Lin, Z. Sun, C. Ma, W. Zhang, S. Chen, H. Wang, Q. Guan, T. Yao, S. Wei, J. Yang, J. Lu, Atomically dispersed iron hydroxide anchored on Pt for preferential oxidation of CO in H₂, Nature 565 (2019) 631–635, https://doi.org/10.1038/s41586-018-0869-5.
- [18] J. Saavedra, T. Whittaker, Z. Chen, C.J. Pursell, R.M. Rioux, B.D. Chandler, Controlling activity and selectivity using water in the Au-catalysed preferential oxidation of CO in H₂, Nat. Chem. 8 (2016) 584–589, https://doi.org/10.1038/ nchem.2494.
- [19] S. Cao, Y. Zhao, S. Lee, S. Yang, J. Liu, G. Giannakakis, M. Li, M. Ouyang, D. Wang, E.C.H. Sykes, M. Flytzani-stephanopoulos, High-loading single Pt atom sites [Pt-O (OH)x] catalyze the CO PROX reaction with high activity and selectivity at mild conditions, Sci. Adv. 6 (2020), eaba3809, https://doi.org/10.1126/sciadv.aha3809.
- [20] S. Sun, D. Mao, J. Yu, Z. Yang, G. Lu, Z. Ma, Lowerature CO oxidation on CuO/ CeO₂ catalysts: the significant effect of copper precursor and calcination temperature, Catal. Sci. Technol. 5 (2015) 3166–3181, https://doi.org/10.1039/ c5cy00124b.
- [21] A.C. Schilling, K. Groden, J.P. Simonovis, A. Hunt, R.T. Hannagan, V. Çınar, J.-S. McEwen, E.C.H. Sykes, I. Waluyo, Accelerated Cu₂O reduction by single Pt atoms at the metal-oxide interface, ACS Catal. 10 (2020) 4215–4226, https://doi.org/10.1021/acscatal.9b05270.
- [22] A.J.R. Hensley, A.J. Therrien, R. Zhang, M.D. Marcinkowski, F.R. Lucci, E.C. H. Sykes, J.-S. McEwen, CO adsorption on the "29" Cu_xO/Cu(111) surface: an integrated DFT, STM, and TPD study, J. Phys. Chem. C 120 (2016) 25387–25394, https://doi.org/10.1021/acs.incc/6b07670
- [23] A.J. Therrien, K. Groden, A.J.R. Hensley, A.C. Schilling, R.T. Hannagan, M. D. Marcinkowski, A. Pronschinske, F.R. Lucci, E.C.H. Sykes, J.S. McEwen, Water activation by single Pt atoms supported on a Cu₂O thin film, J. Catal. 364 (2018) 166–173, https://doi.org/10.1016/j.jcat.2018.04.024.
- [24] J. Shan, N. Janvelyan, H. Li, J. Liu, T.M. Egle, J. Ye, M.M. Biener, J. Biener, C. M. Friend, M. Flytzani-Stephanopoulos, Selective non-oxidative dehydrogenation of ethanol to acetaldehyde and hydrogen on highly dilute NiCu alloys, Appl. Catal. B Environ. 205 (2017) 541–550, https://doi.org/10.1016/j.apcatb.2016.12.045.
- [25] J. Shan, J. Liu, M. Li, S. Lustig, S. Lee, M. Flytzani-Stephanopoulos, NiCu single atom alloys catalyze the C-H bond activation in the selective non-oxidative ethanol dehydrogenation reaction, Appl. Catal. B Environ. 226 (2017) 534–543, https:// doi.org/10.1016/j.apcatb.2017.12.059.
- [26] M.B. Boucher, B. Zugic, G. Cladaras, J. Kammert, M.D. Marcinkowski, T.J. Lawton, E.C.H. Sykes, M. Flytzani-Stephanopoulos, Single atom alloy surface analogs in Pd_{0.18}Cu₁₅ nanoparticles for selective hydrogenation reactions, Phys. Chem. Chem. Phys. 15 (2013) 12187, https://doi.org/10.1039/c3cp51538a.
- [27] J. Liu, F.R. Lucci, M. Yang, S. Lee, M.D. Marcinkowski, A.J. Therrien, C. T. Williams, E.C.H. Sykes, M. Flytzani-Stephanopoulos, Tackling CO poisoning with single-atom alloy catalysts, J. Am. Chem. Soc. 138 (2016) 6396–6399, https://doi.org/10.1021/jacs.6b03339.
- [28] G. Kresse, J. Hafner, Ab initio molecular dynamics for liquid metals, Phys. Rev. B 47 (1993) 558–561, https://doi.org/10.1103/PhysRevB.47.558.
- [29] G. Kresse, J. Furthmüller, Efficient iterative schemes for ab initio total-energy calculations using a plane-wave basis set, Phys. Rev. B - Condens. Matter Mater. Phys. 54 (1996) 11169–11186, https://doi.org/10.1103/PhysRevB.54.11169.
- [30] P.E. Blöchl, Projector augmented-wave method, Phys. Rev. B 50 (1994) 17953–17979, https://doi.org/10.1103/PhysRevB.50.17953.

- [31] G. Kresse, D. Joubert, From ultrasoft pseudopotentials to the projector augmentedwave method, Phys. Rev. B - Condens. Matter Mater. Phys. 59 (1999) 1758–1775, https://doi.org/10.1103/PhysRevB.59.1758.
- [32] J.P. Perdew, K. Burke, M. Emzerhof, Generalized gradient approximation made simple, Phys. Rev. Lett. 77 (1996) 3865–3868, https://doi.org/10.1103/ PhysRevLett.77.3865.
- [33] J.D. Pack, H.J. Monkhorst, "Special points for Brillouin-zone integrations"-a reply, Phys. Rev. B 16 (1977) 1748–1749, https://doi.org/10.1103/PhysRevB.16.1748.
- [34] A.J. Therrien, A.J.R. Hensley, R. Zhang, A. Pronschinske, M.D. Marcinkowski, J.-S. McEwen, E.C.H. Sykes, Characterizing the geometric and electronic structure of defects in the "29" copper surface oxide, J. Chem. Phys. 147 (2017) 224706, https://doi.org/10.1063/1.4996729.
- [35] A.J. Therrien, R. Zhang, F.R. Lucci, M.D. Marcinkowski, A. Hensley, J.S. McEwen, E.C.H. Sykes, Structurally accurate model for the "29"-structure of Cu_xO/Cu(111): a DFT and STM study, J. Phys. Chem. C 120 (2016) 10879–10886, https://doi.org/ 10.1021/acs.jpcc.6b01284.
- [36] G. Henkelman, H. Jónsson, A dimer method for finding saddle points on high dimensional potential surfaces using only first derivatives, J. Chem. Phys. 111 (1999) 7010–7022, https://doi.org/10.1063/1.480097.
- [37] G. Henkelman, B.P. Uberuaga, H. Jónsson, Climbing image nudged elastic band method for finding saddle points and minimum energy paths, J. Chem. Phys. 113 (2000) 9901–9904, https://doi.org/10.1063/1.1329672.
- [38] S.A. Trygubenko, D.J. Wales, A doubly nudged elastic band method for finding transition states, J. Chem. Phys. 120 (2004) 2082–2094, https://doi.org/10.1063/ 1162455
- [39] N. Doudin, S.F. Yuk, M.D. Marcinkowski, M. Nguyen, J. Liu, Y. Wang, Z. Novotny, B.D. Kay, J. Li, V. Glezakou, G. Parkinson, R. Rousseau, Z. Dohnálek, Understanding heterolytic H₂ cleavage and water-assisted hydrogen spillover on Fe₃O₄(001)-supported single palladium atoms, ACS Catal. 4 (2019) 7876–7887, https://doi.org/10.1021/acscatal.9b01425.
- [40] C. Cremers, D. Bayer, F. Jung, T. Jurzinsky, A. Serrov, P. Atanassov, K. Pinkwart, J. Tübke, Palladium alloy catalysts synthesized by sacrificial support method for the electrooxidation of ethylene glycol in alkaline environment, 224th ECS Meet. (2013)
- [41] L. Chen, Y. Zhang, P. Zhu, F. Zhou, W. Zeng, D.D. Lu, R. Sun, C. Wong, Copper salts mediated morphological transformation of Cu₂O from cubes to hierarchical flowerlike or microspheres and their supercapacitors performances, Sci. Rep. 5 (2015) 1–7. https://doi.org/10.1038/srep.09672.
- [42] Y. Yang, D. Xu, Q. Wu, P. Diao, Cu₂O/CuO bilayered composite as a high-efficiency photocathode for photoelectrochemical hydrogen evolution reaction, Sci. Rep. 6 (2016) 1–13, https://doi.org/10.1038/srep35158.
- [43] A. Soon, M. Todorova, B. Delley, C. Stampfl, Thermodynamic stability and structure of copper oxide surfaces: a first-principles investigation, Phys. Rev. B -Condens. Matter Mater. Phys. 75 (2007), 125420, https://doi.org/10.1103/ PhysRevB.75.125420.

- [44] A. Soon, X.Y. Cui, B. Delley, S.H. Wei, C. Stampfl, Native defect-induced multifarious magnetism in nonstoichiometric cuprous oxide: First-principles study of bulk and surface properties of Cu₂₋₈O, Phys. Rev. B - Condens. Matter Mater. Phys. 79 (2009), 035205, https://doi.org/10.1103/PhysRevB.79.035205.
- [45] M.M. Islam, B. Diawara, V. Maurice, P. Marcus, Bulk and surface properties of Cu₂O: a first-principles investigation, J. Mol. Struct. Theochem. 903 (2009) 41–48, https://doi.org/10.1016/j.theochem.2009.02.037.
- [46] L.Y. Isseroff, E.A. Carter, Importance of reference Hamiltonians containing exact exchange for accurate one-shot GW calculations of Cu₂O, Phys. Rev. B - Condens. Matter Mater. Phys. 85 (2012), 235142, https://doi.org/10.1103/ PhysRevB 85 235142
- [47] C.H. Kuo, C.H. Chen, M.H. Huang, Seed-mediated synthesis of monodispersed Cu₂O nanocubes with five different size ranges from 40 to 420 nm, Adv. Funct. Mater. 17 (2007) 3773–3780, https://doi.org/10.1002/adfm.200700356.
- [48] J. Shan, F.R. Lucci, J. Liu, M. El-Soda, M.D. Marcinkowski, L.F. Allard, E.C. H. Sykes, M. Flytzani-Stephanopoulos, Water co-catalyzed selective dehydrogenation of methanol to formaldehyde and hydrogen, Surf. Sci. 650 (2016) 121–129, https://doi.org/10.1016/j.susc.2016.02.010.
- [49] F.R. Lucci, J. Liu, M.D. Marcinkowski, M. Yang, L.F. Allard, M. Flytzani-Stephanopoulos, E.C.H. Sykes, Selective hydrogenation of 1,3-butadiene on platinum-copper alloys at the single-atom limit, Nat. Commun. 6 (2015) 8550, https://doi.org/10.1038/ncomms9550.
- [50] J. Jones, H. Xiong, A.T. DeLaRiva, E.J. Peterson, H. Pham, S.R. Challa, G. Qi, S. S. Oh, M.H. Wiebenga, X.I. Pereira Hernandez, Y. Wang, A.K. Datye, X.I. P. Hernández, Y. Wang, A.K. Datye, Thermally stable single-atom platinum-on-ceria catalysts via atom trapping, Science 353 (2016) 150–154, https://doi.org/10.1126/science.aaf8800
- [51] Y.F. Han, M.J. Kahlich, M. Kinne, R.J. Behm, Kinetic study of selective CO oxidation in H₂-rich gas on a Ru/γ-Al₂O₃ catalyst, Phys. Chem. Chem. Phys. 4 (2002) 389–397, https://doi.org/10.1039/b103780n.
- [52] D. Teschner, A. Wootsch, O. Pozdnyakova-Tellinger, J. Kröhnert, E.M. Vass, M. Hävecker, S. Zafeiratos, P. Schnörch, P.C. Jentoft, A. Knop-Gericke, R. Schlögl, Partial pressure dependent in situ spectroscopic study on the preferential CO oxidation in hydrogen (PROX) over Pt/ceria catalysts, J. Catal. 249 (2007) 318–327, https://doi.org/10.1016/j.jcat.2007.05.010.
- [53] G. Sedmak, S. Hočevar, J. Levec, Kinetics of selective CO oxidation in excess of H₂ over the nanostructured Cu_{0.1}Ce_{0.9}O_{2-y} catalyst, J. Catal. 213 (2003) 135–150, https://doi.org/10.1016/S0021-9517(02)00019-2.
- [54] A. Siani, B. Captain, O.S. Alexeev, E. Stafyla, A.B. Hungria, P.A. Midgley, J. M. Thomas, R.D. Adams, M.D. Amiridis, Improved CO oxidation activity in the presence and absence of hydrogen over cluster-derived PtFe/SiO₂ catalysts, Langmuir 22 (2006) 5160–5167. https://doi.org/10.1021/ja053476a.
- [55] K. Ding, A. Gulec, A.M. Johnson, N.M. Schweitzer, G.D. Stucky, L.D. Marks, P. C. Stair, Identification of active sites in CO oxidation and water-gas shift over supported Pt catalysts, Science 350 (2015) 189–192, https://doi.org/10.1126/science.aac6368.